Ostwald Ripening in Systems with Competing Interactions

Celeste Sagui and Rashmi C. Desai
Department of Physics, University of Toronto, Toronto, Ontario M5S 1A7, Canada
(Received 2 September 1994)

We study the effects of a long-range repulsive interaction on the classical coarsening mechanism of Lifshitz and Slyozov. Beginning with a Langevin description, a set of interface equations describing both the growth and motion of droplets is derived and solved numerically. We study two regimes: in one, the system reaches hexagonal order and the droplet distribution function becomes a delta function; in the other, the system is disordered and polydisperse with a strong coupling between the position and the size of the droplets.

PACS numbers: 61.20.Ja, 64.60.–i, 64.75.+g, 75.70.Kw

Ostwald ripening is the process by which droplets of a minority phase in a binary mixture coarsen during the late stages of phase separation. In order to maintain local equilibrium, material from small, high curvature droplets evaporate, diffuse through the matrix, and condense onto the nearby large, low curvature droplets. The interfacial free energy of the system is thereby reduced. This mechanism was first described by Lifshitz, Slyozov, and Wagner (LSW) [1] in the limit of zero volume fraction. They showed that a scaling regime is reached, wherein the mean droplet radius increases as a power law with growth exponent of 1/3, and derived an expression for the scaled droplet distribution function. Since their seminal paper, there has been extensive experimental, analytical, and numerical work on the LSW mechanism [2].

The LSW mechanism describes systems with a conserved order parameter and attractive interactions only. However, there is a significant class of materials characterized by both short-range attractive and effective long-range repulsive interactions (LRRI). Such systems typically form modulated structures of a specific size and spatial distribution. Important examples include Langmuir monolayers [3], block-copolymer systems [4], ferrofluids [5], and charged colloidal suspensions [6].

In this Letter, we present a general treatment of the coarsening mechanism appropriate for systems with LRRI. Starting from a Ginzburg-Landau free energy description, we derive a set of equations describing both the growth and motion of the minority phase droplets. In most cases, the system reaches hexagonal order and the droplet distribution function evolves from a broad, flat function to a delta function, as the droplets approach their equilibrium size. However, it is possible to find steady-state regimes characterized by polydispersity; the size of the droplets depends on coordination number. Two such polydisperse states are discussed: in one the system is kinetically frozen; in the other the system evolves with a growth exponent $n < 1/3$.

We begin with the appropriate free energy functional, written in terms of the order parameter ϕ. It contains both an attractive square gradient and a long-range repulsive term [7]. In dimensionless form,

$$F\{\phi\} = \int d^d r \left[\tfrac{1}{2}(\nabla\phi)^2 + f(\phi)\right] + \frac{\beta'}{2}\int\int d^d r\, d^d r'\, \phi(\mathbf{r}) g(|\mathbf{r} - \mathbf{r}'|)\phi(\mathbf{r}'), \tag{1}$$

where $g(|\mathbf{r} - \mathbf{r}'|)$ is the kernel of the LRRI of relative strength β'. In this dimensionless form, coordinates are expressed in terms of a characteristic length ξ proportional to the interface thickness. The local free energy per site has a double-well structure, $f(\phi) = -\frac{1}{2}\phi^2 + \frac{1}{4}\phi^4$, for temperatures below the critical temperature. For definiteness, we have chosen to study the 2D kernel $g(|\mathbf{r} - \mathbf{r}'|) = |\mathbf{r} - \mathbf{r}'|^{-1} - [(\mathbf{r} - \mathbf{r}')^2 + L^2]^{-1/2}$, appropriate for a Langmuir monolayer of thickness L [8]. The equilibrium phase diagrams for fixed values of L and β' are known: The system exhibits modulated stripe and hexagonal phases as a function of the mean concentration ϕ_0.

The time evolution of the system after a quench from the high-temperature disordered phase is given by the Langevin equation

$$\partial\phi(\mathbf{r}, t)/\partial t = \nabla^2\, \delta F/\delta\phi, \tag{2}$$

where we neglect thermal noise. Numerical studies of the Langevin equation show, that after a quench into the hexagonal phase, a long-wavelength instability creates a morphology of interpenetrating domains. Inside these domains, the order parameter saturates at $\phi_{\text{bulk}} = \pm\phi_{\text{sat}}$. The system then undergoes a series of early-time shape changes that leads it to a disordered, liquidlike state of minority-phase droplets of varying sizes. During its late stages, the system continues to evolve via the growth and dissolution of droplets and the elimination of defects. In most cases, a final monodisperse state of droplets with a spatially triangular distribution is reached. We shall show that the system can also behave as a polydisperse liquid, with a quasiconstant concentration of defects.

Starting with the Langevin equation [9], we have used the method of matched asymptotic expansions [10] to

0031-9007/95/74(7)/1119(4)$06.00

obtain a macroscopic description of interfacial dynamics. The expansion parameter is proportional to the ratio of the interfacial width to a typical macroscopic length, determined by the curvature. To *first order*, we obtain three coupled equations. First, a quasistatic approximation for the order parameter in the bulk, $\partial\phi/\partial t = 0$, or equivalently, $\nabla^2[\mu_{\mathrm{LSW}} + \beta' \int d^d r' g(|\mathbf{r} - \mathbf{r}'|)\phi_{\mathrm{bulk}}(\mathbf{r}')] = 0$, where μ_{LSW} is the classical chemical potential, $\mu_{\mathrm{LSW}} = 2[\phi(\mathbf{r}) - \phi_{\mathrm{bulk}}]$. Second, the boundary condition for μ_{LSW} at the interface I of a droplet of radius R: $\mu_{\mathrm{LSW}}|_I = \{(d-1)\sigma/2\phi_{\mathrm{sat}}R\}$, where σ is the local surface tension. Third, the equation for the normal velocity $\dot{R}$ of the interface, proportional to the discontinuity of μ_{LSW} across the interface: $2\phi_{\mathrm{sat}}\dot{R} = [\hat{\mathbf{n}} \cdot \nabla\mu_{\mathrm{LSW}}]_I$. We rescale length and time by the dimensionless capillary length $l_c = (d-1)\sigma/4\phi_{\mathrm{sat}}^2$, i.e., $\mathbf{x} = \mathbf{r}/l_c$ and $\tau = t/l_c^2$. The local chemical potential is $\mu(\mathbf{x}) = 2\phi_{\mathrm{sat}}\theta(\mathbf{x})$, where $\theta(\mathbf{x})$ is given by

$$\theta(\mathbf{x}) = \frac{\phi(\mathbf{x}) - \phi_{\mathrm{bulk}}}{\phi_{\mathrm{sat}}} + \beta \sum_{i=1}^{N} \int_{D_i} d^d x_i' \, g(|\mathbf{x} - \mathbf{x}_i'|) . \tag{3}$$

Here, N is the number of droplets of the system, D_i is a spherical domain of radius R_i, and β is rescaled β'. The integration of the interface equations gives a steady-state multidroplet diffusion equation in the form of a Poisson equation for $\theta(\mathbf{x})$ with a surface charge on droplet i proportional to $-\dot{R}_i$ [11,12]. In the monopole approximation [13], the multidroplet diffusion equation becomes

$$\nabla^2\theta(\mathbf{x}) = a \sum_{i=1}^{N} B_i \delta(\mathbf{x} - \mathbf{X}_i) , \tag{4}$$

where $a = 2\pi^{(d/2)}/\Gamma(d/2)$, $\mathbf{X}_i$ is the center of mass of droplet i, and B_i is the strength of the source or sink of current for diffusion. On the surface of droplet i, $\theta(\mathbf{x})$ is

$$\theta(\mathbf{x})|_{|\mathbf{x}-\mathbf{X}_i|=R_i} = I_{\mathrm{LSW}} + I_{\mathrm{intra}} + I_{\mathrm{inter}} , \tag{5}$$

where $I_{\mathrm{LSW}} = 1/R_i$ is the LSW contribution to the chemical potential, $I_{\mathrm{intra}} = \beta \int_{D_i} d^d x_i' \, g(|\mathbf{R}_i - \mathbf{x}_i'|)$ is the intradomain term, and $I_{\mathrm{inter}} = \beta \sum_{j\neq i} \int_{D_j} d^d x_j' \, g(|\mathbf{R}_i - \mathbf{x}_j'|)$ is the interdomain term. We call V_{LSW}, V_{intra}, and V_{inter} the resulting growth rates.

The mass balance equation is

$$d(vR_i^d)/d\tau = -\int_{S_i} \mathbf{j} \cdot \hat{\mathbf{n}} \, dS , \tag{6}$$

where $v = a/d$, S_i is the surface of the ith droplet, $\hat{\mathbf{n}}$ is the unit vector normal to the droplet surface, and $\mathbf{j} = -\nabla\theta(\mathbf{x})$ is a mass flux density with a purely diffusive term and a term due to the LRRI. The evaluation of this flux on the droplet surface S_i gives the growth law

$$R_i^{d-1} \, dR_i/d\tau = B_i . \tag{7}$$

Conservation of the total flux in the system requires

$$\sum_{i=1}^{N} B_i = 0 . \tag{8}$$

Equations (4) to (8) describe the growth of the droplets, and in the absence of the LRRI, when applied to spherical precipitates, they reduce to those of the LSW mechanism with a finite volume fraction [14]. However, in systems with a LRRI, these must be augmented by an equation describing the translation of droplets, since they assume a specific spatial pattern. The integration of the interface equations, assuming that the deformation from sphericity is negligible [11,13], gives a Langevin equation for $\mathbf{X}_i$:

$$\frac{d\mathbf{X}_i}{d\tau} = -\frac{M\beta}{vR_i^d} \sum_{\substack{j=1 \\ j\neq i}}^{N} \nabla_i \int_{D_i} d^d r_i \int_{D_j} d^d r_j' \, g(|\mathbf{X}_{ij} + \mathbf{r}_{ij}|) , \tag{9}$$

where $\mathbf{X}_{ij} = \mathbf{X}_i - \mathbf{X}_j$, $\mathbf{r}_{ij} = \mathbf{r}_i - \mathbf{r}_j'$, and M/vR_i^d is the mobility. The motion is given by the interdomain contribution, i.e., the positioning of surrounding droplets, mediated through the LRRI. The integration of the interface equations gives $M = 1$. We treat M as a phenomenological parameter in order to study the effects of enhancing or hindering hexagonal order and to allow for different modes of mass transport for different LRRI systems.

The above equations constitute a formal solution of the LSW problem for systems with LRRI. The advantage of this approach, over Eqs. (1) and (2), is that one can study each of the factors in Eq. (5) independently and also study long-time behavior with less computing time. To solve these equations, a generalization of the numerical technique previously described in the literature [14] was used. The 2D system was initialized by generating a random set of $\{R_i\}$ and a set of centers of mass $\{\mathbf{X}_i\}$ (without droplet overlap). Next, Eq. (4) was solved using Eq. (5) for the set of $\{B_i\}$, subject to the conservation law Eq. (8). Then Eqs. (7) and (9) were integrated numerically using an Euler discretization scheme. This generated a new set of $\{R_i\}$ and $\{\mathbf{X}_i\}$, and the process was iterated [15]. Generally, our simulations began with $N_0 = 500$ disks, distributed either at random or in a triangular lattice in a rectangular box which requires an equilibrium number of droplets $N_{\mathrm{eq}} \leq N_0$. We varied the film thickness, $0.1 \leq L \leq 10$, and for each L we tried different values of β, for volume fractions $0.02 \leq \phi_0 \leq 0.40$ [13]. The parameter M, which sets the relative time scale of the triangular ordering of the droplets to the LSW mechanism, was also varied. During the simulation, the average radius and the droplet distribution function were computed. The evolution of the spatial distribution of the droplets and the processes of topological defect annihilation were studied and analyzed using standard Voronoi construction techniques.

The left column in Fig. 1 shows the effects of both the spatial and size distributions of the droplets on the coarsening rates V_{LSW}, V_{intra}, V_{inter}, and V_T ($V_T = \dot{R} = V_{\mathrm{LSW}} + V_{\mathrm{intra}} + V_{\mathrm{inter}}$). Both V_{LSW} and V_{intra} are independent of

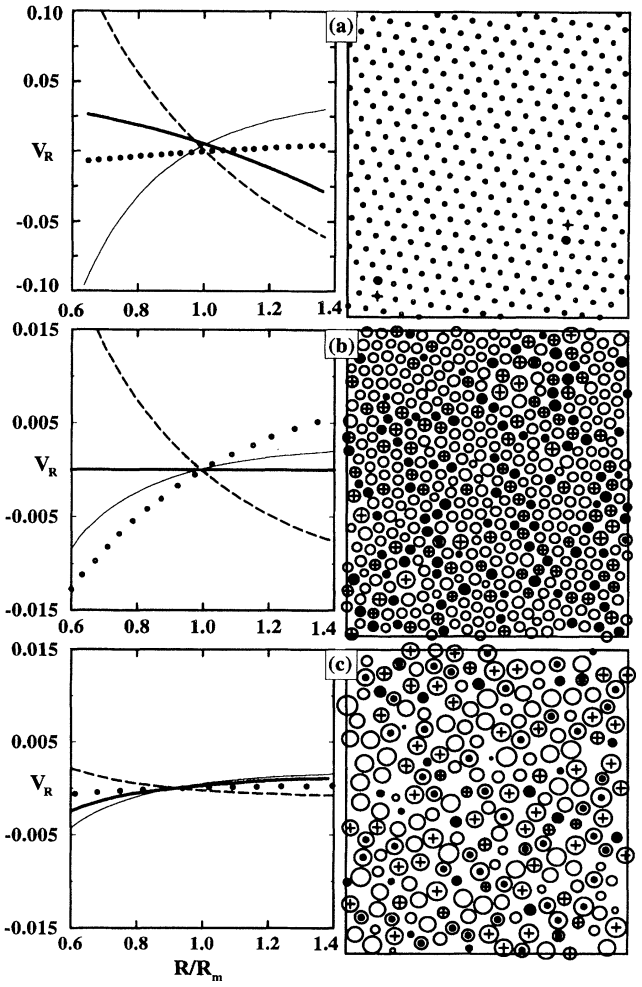

FIG. 1. Right column shows configurations for (a) a monodisperse system in the triangular crystalline state ($L = 10, \beta = 0.36, \phi_0 = 0.04, M = 1, \tau \sim 170\,000$); (b) a system frozen in a polydisperse liquid state ($L = 10, \beta = 0.08, \phi_0 = 0.40, M = 0.001, \tau \sim 544\,000$); (c) a polydisperse coarsening system ($L = 2.5, \beta = 0.08, \phi_0 = 0.40, M = 4, \tau \sim 6000$). Droplets with coordination number $z < 6$ are indicated with filled disks and those with $z > 6$ with a plus sign. The crystalline configuration has a pair of dislocations. Left column shows the growth rate distributions V_R. Thin solid line: V_{LSW}; dashed line: V_{intra}; dots: V_{inter}; thick solid line: V_T. (a) Contributions for *initial* random radii and random coordinates: V_{inter} and thus also V_T produce a very disperse cloud of dots; here only their *averages* are shown. (b) Contributions for the frozen configuration. (c) Contributions for the coarsening system.

coordinates, while V_{inter} depends crucially on them. Consider a broad radius distribution. V_{LSW} describes the classical situation in absence of LRRI ($\beta = 0$), i.e., droplets with radii smaller than the mean radius R_m have negative growth rates and shrink, while droplets with $R > R_m$ grow. V_{intra} has the opposite behavior: droplets with $R < R_m$ have positive growth rates, while those with $R > R_m$ have negative rates; this term favors a monodisperse droplet distribution. If the radii are chosen uncorrelated 1(a), V_{inter} produces a disperse cloud of points; its dispersion increases with volume fraction or with randomness of coordinates. Individual droplet points in the uncorrelated V_{inter} distribution may have any growth rate, depending on their immediate environment. For a strongly correlated system 1(b) and 1(c), on the other hand, V_{inter} produces a well-defined curve. In both cases, the average V_{inter}, like V_{LSW}, gives a mass flux from smaller to larger particles. A minimization of the droplet free energy shows that if $\beta L^2 > 0.98\sigma(\phi_0)$ then the equilibrium radius R_{eq} is finite ("noncoarsening" solution). The function $\sigma(\phi_0)$ originates in the interaction term and is a monotonically increasing function of ϕ_0, with $\sigma(0) = 1$. It has been computed for a dipolar interaction by McConnell [16]. If the system is free to reach hexagonal order, $V_{\mathrm{intra}} > -(V_{\mathrm{LSW}} + V_{\mathrm{inter}})$, and the resulting V_T leads the system to a monodisperse distribution 1(a). This behavior occurs for any mobility $M \geq 0.01$. However, if the hexagonal order is hindered, for instance by taking the limit $M \to 0$, then $V_{\mathrm{intra}} = -(V_{\mathrm{LSW}} + V_{\mathrm{inter}})$. The system becomes kinetically frozen in a polydisperse configuration 1(b). If $\beta L^2 < 0.98\sigma(\phi_0)$, $R_{\mathrm{eq}} \to \infty$, and $V_{\mathrm{intra}} < -(V_{\mathrm{LSW}} + V_{\mathrm{inter}})$. The system coarsens and is polydisperse 1(c), independently of the value of M. The tendency of V_{intra} to produce a monodisperse distribution and of V_{inter} to produce a strong coupling between the position and size of droplets are new features absent in the classical LSW mechanism.

The right column in Fig. 1 shows configurations for (i) noncoarsening systems in (a) the crystalline state and (b) a frozen polydisperse liquid state; (ii) a coarsening system 1(c). In Fig. 1(a) the droplets evolved from an initial state, where random coordinates and random radii produce the velocity distribution shown, to a final configuration with equal radii and triangular coordinates ($V_T = 0$), except for a few dislocations [17]. The mechanisms of defect annihilation and collision are as reported in a Langevin simulation study [7]. For systems such as those shown in 1(b) the concentration of defects stays almost constant. In the noncoarsening case, the hexagonal order contributes to the achievement of monodispersity. Systems with slow mobilities far from the triangular configuration can be stabilized with $V_T = 0$ for a wide range of R through the coupling between defects and the size of the constitutive droplets. In the coarsening case 1(c), the coupling of topological disorder and polydispersity contained in V_{inter} stabilizes the system as an *evolving* froth [18]. This case resembles the experimental results obtained for an amphiphilic monolayer by Seul and co-workers [18].

Figure 2(a) shows the average droplet distribution as function of R/R_m. The delta function corresponds to monodisperse triangular systems 1(a), the symmetric peak to frozen systems 1(b), and the one resembling a classical distribution corresponds to the coarsening systems 1(c). The inset shows the normalized mean area, $x_z = \langle A_z \rangle / \langle A \rangle$, of z-fold coordinated droplets for 1(b) and 1(c). Figure 2(b) shows the dependence of the average radius R_m

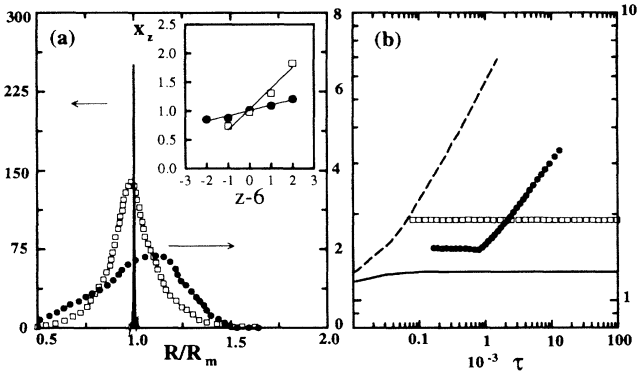

FIG. 2. Solid line: parameters of Fig. 1(a). Open squares: parameters of Fig. 1(b). Filled circles: parameters of Fig. 1(c). (a) Average droplet distribution function $f(R/R_m)$. The left scale is for the delta function and the right for the spread functions. The inset shows x_z as defined in the text. (b) Average radius R_m as a function of time. Dashed line: classical LSW result ($\phi_0 = 0.04$). Curves displaced with respect to each other for clarity.

on time. The classical LSW result has a growth exponent $n = 1/3$. For 1(a), the growth of R_m stops once the delta function is reached. For 1(b), R_m is also constant, while $R_m \sim t^n$ in 1(c), with $n = 0.29$.

The magnitude of hexagonal order present in early stages stabilizes noncoarsening systems against the LSW mechanism. In a random radius distribution with triangular coordinates (and low volume fractions), V_{inter} is a narrow band around $V_R = 0$, so that V_T is positive for $R < R_m$ and negative for $R > R_m$. For random coordinates, V_{inter} is very disperse and many small droplets in the cloud have very negative V_T. In a simulation with an initial triangular configuration with random radii the final monodisperse state has a number of droplets equal to the initial one. If the process is repeated exactly but with random initial coordinates, the system eliminates several droplets before the radius distribution becomes a delta function. In both cases, the final configuration is triangular, but in the first case the resulting lattice constant is smaller. Keeping everything the same, but varying M, produces similar results. A large mobility sets the hexagonal order sooner so that such systems are stabilized sooner against the LSW mechanism and, therefore, their final number of droplets is higher.

In summary, we studied the effects of a LRRI on the LSW mechanism. Starting from the Langevin description, a set of interface equations which couple growth and motion of droplets was derived. We found a noncoarsening and a coarsening regime. In the noncoarsening regime, the system is history dependent and sensitive to the magnitude of the hexagonal order present in the early stages. Monodispersity is aided by hexagonal order. If hexagonal order is hindered, the system is stabilized—through the coupling produced by I_{inter} between the positions and sizes of droplets—as a kinetically frozen polydisperse liquid, where the mean radius is constant in time. In the coarsening regime, the coupling of topological disorder and polydispersity stabilizes the system as an *evolving* froth that coarsens with a reduced growth exponent.

We wish to thank J. H. Yao, M. Seul, and Chuck Yeung for useful discussions. This work was supported by the NSERC of Canada.

[1] I. M. Lifshitz and V. V. Slyozov, J. Phys. Chem. Solids **19**, 35 (1961); C. Wagner, Z. Electrochem. **65**, 581 (1961).
[2] J. A. Marqusee and J. Ross, J. Chem. Phys. **80**, 536 (1984); P. W. Voorhees, J. Stat. Phys. **38**, 231 (1985); C. W. J. Beenaker, Phys. Rev. A **33**, 4482 (1986); Y. Enomoto, M. Tokuyama, and K. Kawasaki, Acta Metall. **34**, 2119 (1986); M. Marder, Phys. Rev. A **36**, 858 (1987); A. J. Ardell, Phys. Rev. B **41**, 2554 (1990); J. H. Yao, K. R. Elder, H. Guo, and M. Grant, Phys. Rev. B **45**, 8173 (1992).
[3] H. M. McConnell, Annu. Rev. Phys. Chem. **42**, 171 (1991).
[4] L. Leibler, Macromolecules **13**, 1602 (1980); T. Ohta and K. Kawasaki, Macromolecules **19**, 2621 (1986); Y. Oono and M. Bahiana, Phys. Rev. Lett. **61**, 1109 (1988).
[5] R. E. Rosensweig, M. Zahn, and R. Shumovich, J. Magn. Magn. Mater. **39**, 127 (1983).
[6] C. A. Murray and D. H. Van Winkle, Phys. Rev. Lett. **58**, 1200 (1987).
[7] C. Sagui and R. C. Desai, Phys. Rev. Lett. **71**, 3995 (1993); C. Sagui and R. C. Desai, Phys. Rev. E **49**, 2225 (1994).
[8] D. Andelman, F. Brochard, and J. F. Joanny, J. Chem. Phys. **86**, 3673 (1987).
[9] For the late stages it is irrelevant if droplets formed through nucleation or spinodal decomposition.
[10] K. Kawasaki and T. Ohta, Physica (Amsterdam) **118A**, 175 (1983); R. L. Pego, Proc. R. Soc. London A **422**, 261 (1989); G. Caginalp, Ann. Phys. (N.Y.) **172**, 136 (1986).
[11] C. Sagui and R. C. Desai (to be published).
[12] N. Akaiwa and P. W. Voorhees, Phys. Rev. E **49**, 3860 (1994).
[13] The monopole approximation implies small volume fractions. Larger volume fractions generate distortions of the spherical shape that translate into particle migration [12]. In our case, the LRRI stabilizes the spherical shape and is the main cause of particle motion, so we expect this approximation to be valid for higher volume fractions.
[14] P. W. Voorhees and M. E. Glicksman, Acta Metall. **32**, 2001 (1984); 2013 (1984); J. H. Yao, K. R. Elder, H. Guo, and M. Grant, Phys. Rev. B **47**, 14 110 (1993).
[15] If, in any time step, the result of the growth in R or of the coordinate motion is the overlap of two droplets, then we allow them to coalesce. Coalescence events are very rare.
[16] H. M. McConnell, Proc. Natl. Acad. Sci. **86**, 3452 (1989). For our interaction, $\sigma(\phi_0)$ also depends weakly on the film thickness.
[17] In some runs, the formation of grain boundaries which disrupt the hexagonal order is also observed.
[18] M. Seul and C. A. Murray, Science **262**, 558 (1993); M. Seul, N. Y. Morgan, and C. Sire, Phys. Rev. Lett. **73**, 2284 (1994); N. Y. Morgan and M. Seul (to be published); C. Sire and M. Seul (to be published).